

A Nondestructive Approach to Evaluating Impact Damaged Composite Structures

Hyonny Kim, Keith T. Kedward

Department of Mechanical and Environmental Engineering
University of California at Santa Barbara
Santa Barbara, California 93106, USA

Summary: The challenge of assessing impact damage with regard to the global function of load bearing components represents a long standing issue for composite technologies. Four Point Bending stiffness tests are used to evaluate the effect of high velocity ice impact damage on the performance of minimum gauge structures. As the design of such structures is often driven by global buckling considerations, and since buckling is a stiffness dependent failure mode, knowledge of the reduction in bending stiffness due to impact damage and the ability to predict this reduction is of practical interest. A simple mechanics based methodology used for estimating reduction in bending stiffness is applied to predict critical buckling load for impact damaged plates. Results show a near 1:1 correlation between predicted reductions in bending stiffness and critical buckling load. This suggests that for initial assessments, four point bending tests may be performed instead of more complicated buckling tests.

Keywords: Post Impact Evaluation, Nondestructive Evaluation, Damage Tolerance, Buckling Prediction, Composite Structure Design, Strip Methods

Introduction

In the evaluation of load bearing structures, one must consider strength as well as stiffness-influenced structural characteristics such as stability and vibration. Structures designed for minimum weight, thus often for minimum gauge thickness, are commonly found in the aerospace industry. When such structures are subjected to compressive loading, the stability of these structures must be assessed. Examples of such structures are stringer-stiffened fuselage airframes and fan cowls surrounding large modern gas turbine engines. Many of these thin gauge composite structures are situated such that they are susceptible to foreign object impact damage. While the design of a damage resistant structure is favorable for maintenance related and many other reasons (most all associated with costs), current certification methodology dictates the design of structures such that they tolerate an acceptable amount of impact damage while still meeting specific performance requirements (please note the difference between damage tolerant and damage resistant structures; Sjöblom [1]). In structures which are buckling critical design, the existence of impact damage can potentially result in a significant reduction in performance. Alternatively, the inclusion of

impact damage in a structure's design results in a structure of increased weight in order to satisfy damage tolerance requirements. The question of how much additional weight will the structure need to gain now arises. Thus the ability to predict the effect of impact damage on the performance of a structure is of significant interest.

Conventional two dimensional composite structures, while exhibiting potentially outstanding performance in the lamina plane, are vulnerable when subjected to modes of loading challenging the material in the out-of-plane direction. Foreign object impacts present a composite structure with an extremely complex loading state, especially in the case of high velocity impacts where dynamics need to be accounted for. Often impact damage creates what industry terms as Barely Visible Impact Damage (BVID). BVID comes in the form of intraply cracking, delaminations, and backside fiber failure.

The detection of BVID requires painstaking attention as it usually involves physical contact between a technician and the hardware. Due to the difficulty in detecting BVID, the designer must take into account the fact that the structure shall be expected to perform with BVID present. This account would be introduced at the design stage of the structure and shall ultimately be verified with a mechanical test of the entire structure. In order to assess whether a structure can functionally tolerate damage, simplified methods of analyses need to be available to the designer. These design methods, preferably based on fundamental mechanics, provide designers with a tool by which to scale specific structural parameters as well as take into account various damage zone sizes. This activity would be introduced at the design stage where decisions are much less costly than those made as one progresses towards the final completion of a product [2].

A method for predicting the reduction in bending stiffness and global buckling critical load has been developed. This method treats thin gauge plates with length to thickness ratios on the order of 100:1 and assumes global buckling as initial failure mode under in-plane compression. It is hypothesized that this mode of failure remains prevalent even for structures sustaining moderate forms of BVID, such as large delaminations.

While most aircraft structures contain some degree of curvature, the research presented here investigates flat plates. The treatment of flat plates is intended to serve as a foundation for which methods developed can be extended to curved shells. Several authors have performed meaningful investigations on the buckling of curved composite shells [3,4].

Impact Tests

High velocity impact tests have been performed on a series of flat 304.8 mm square composite plates [5]. The composite plates tested, summarized in Table 1, are AS4 fabric (5 and 8 harness satin weaves) with toughened 977 and 8552 resin systems. A progression of damage modes, illustrated in Figure 1, has been identified for each type of specimen with a clear distinction found between modes resulting in Visible Impact Damage (VID) and those resulting in BVID. All damage was produced by the high velocity impact of simulated hail ice spheres onto the targets which were held in a frame with rotationally (but not extensionally) fixed boundaries. The spheres constructed of multiple layers oriented in flat planes perpendicular to the direction of travel were 25.4 to 50.8 mm in diameter and were projected at speeds ranging from 30 to 200 m/sec. by a nitrogen gas cannon.

Of present interest are the BVID modes. Damage modes classified as Types I and II in Figure 1 are forms in which no target penetration occurred and BVID resulted. On pertinent panels, the delamination patterns have been mapped out by the ever-popular "quarter-tap" method as well as by hand held ultrasonic inspection methods.

Table 1. Carbon Fabric/Epoxy Composite Panel Test Matrix

Series ID	Material	Layup	Thk. (mm)	Qty.
ICE-01	AS4/977 5HS	[0/45/90] _s	1.42	3
ICE-02	AS4/977 5HS	[0/45/90/-45] _s	1.91	3
ICE-03	AS4/977 5HS	[0/45/90/-45/0/45] _s	2.62	2
ICE-04	AS4/8552 8HS	[0/45] _s	1.22	16
ICE-05	AS4/8552 8HS	[0/45/90] _s	1.83	6
ICE-06	AS4/8552 8HS	[0/45/90/-45] _s	2.44	6

Total: 36

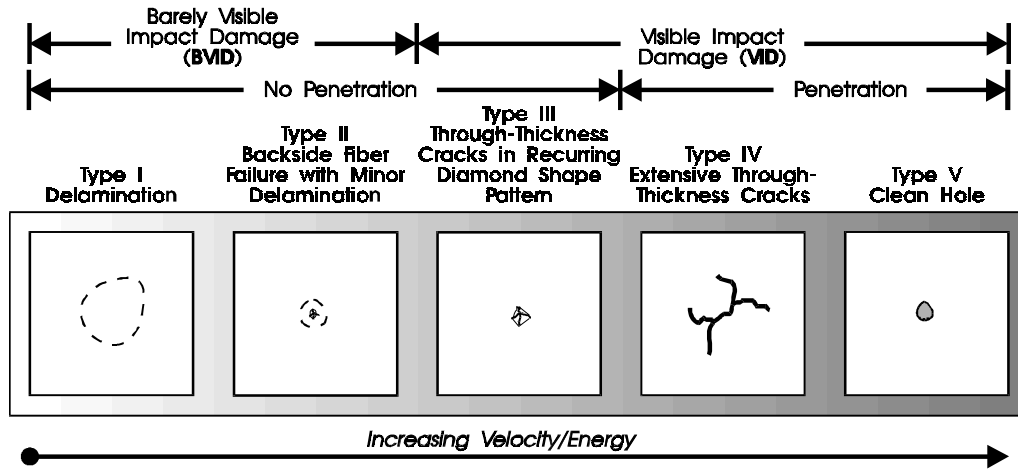


Figure 1. Failure Mode Progression Observed in Ice Impact Testing

Four Point Bending Tests

Four Point Bending (FPB) tests have been used to evaluate the effect of impact damage on thin gauge composite structures. The decision for using this test instead of the more popular Compression After Impact (CAI) test was made based on the nature of the structures being considered. As discussed, the global buckling of thin gauge structures is directly dependent on the plate bending stiffness. Thus, knowledge of the reduction in bending stiffness due to impact damage and the ability to predict this reduction is of significant interest when designing buckling critical structures.

The FPB geometry was selected due to one's ability to apply a field of constant moment and zero interlaminar shear force across a zone of damage on a composite panel. Many researchers have investigated the use of bending tests to evaluate the strength of composites. However, as pointed out by Wisnom [6] and Grédiac [7], there exists many inherent limitations when flexure tests are used to assess strength. Adler and Mihora [8] have used a related bending test (concentric ring-on-ring producing constant radial moment) to evaluate the effects of impact damage on circular ceramic plates.

A FPB test fixture for measuring stiffness has been configured such that load and support points do not interfere with zones of damage. For the 304.8 mm square panels, a support-span of $L = 279.4$ mm and a load-span to support-span ratio of 9:11 ($b = 25.4$ mm in Figure 3) was used. Polished stainless steel cylindrical bars were used for the support and loading noses. All ice impact test panels listed in Table 1 have been tested with this four point test fixture and the reduction in bending stiffness, albeit under this specific geometry,

have been measured. These measurements for the panels containing delamination damage shall be discussed further below and are presented in Table 2.

Predictive Methodology

A simple mechanics based method has been developed which accurately predicts the reduced bending stiffness for the delamination damaged panels under investigation. Detailed in Figure 2, this analysis consists of considering a delaminated plate which is theoretically decomposed into several strips. Pertinent strips contain sections along their length having different bending properties. An example of modeling a plate using eight strips to define a delamination zone is also shown in the figure. The stiffness under the applied FPB loading is determined for each strip separately using simple beam bending theory. As shown in Figure 2, strips which account for damage are modeled in three discrete sections, with the central section having a different plate bending stiffness D_2 (isotropic plate bending stiffness $D = \frac{Et^3}{12(1-\nu^2)}$) than the undamaged sections D_1 (with $D_2 < D_1$).

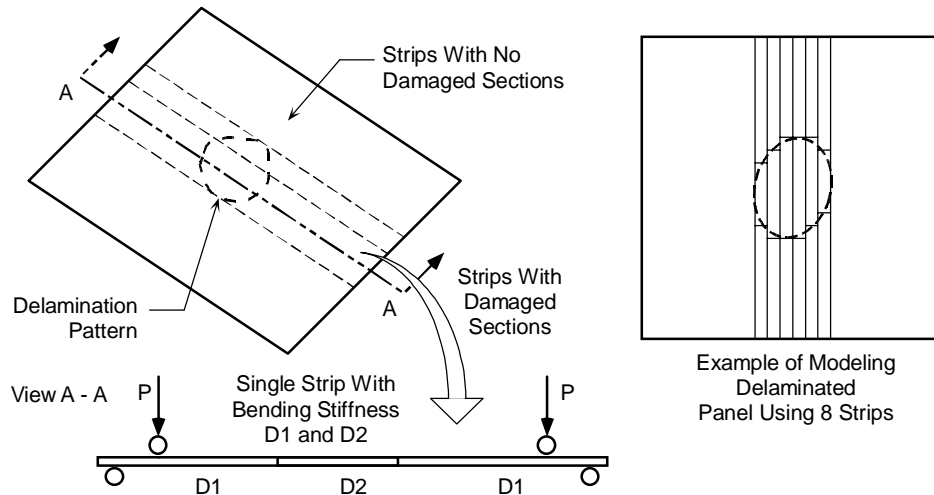


Figure 2. Strip Based Approach to Modeling Delaminated Panel

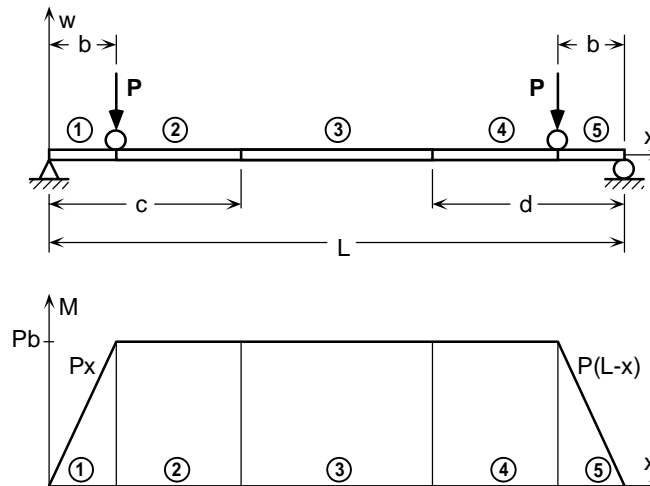


Figure 3. Simple Beam Model and Moment Diagram

The beam bending model of these multisectioned strips is detailed in Figure 3. For a general plate strip, we assume one-dimensional beam bending behavior:

$$\frac{d^2w_i}{dx^2} = \frac{M_i}{D_i} \quad i=1, 2, \dots, 5 \quad (1-5)$$

Where i ranges from 1 to 5 to account for each beam section as shown in Figure 3. w_i are the transverse displacement functions with corresponding plate bending stiffness constants D_i for each section of the plate strip. In general, $D_1 = D_2 = D_4 = D_5$ and $D_3 < D_1$. In modeling the delaminated region, the assumption is made that a single delamination exists at the geometric midplane, yielding $D_3 = D_1/4$ (treat as split beam). As the beam is a one-dimensional problem, D_{11} from the Classical Lamination Plate Theory “D” matrix is used for values of D_i . The moments, as shown in Figure 3 are:

$$M_1 = Px \quad M_2 = M_3 = M_4 = Pb \quad M_5 = P(L-x) \quad (6)$$

Integration of Eqns 1 to 5 yield 10 unknown constants which are solved for by application of boundary and continuity conditions:

$$\text{Boundary Conditions:} \quad w_1(0) = w_5(L) = 0 \quad (7)$$

$$\begin{aligned} \text{Continuity:} \quad w_1(b) &= w_2(b) & \frac{dw_1(b)}{dx} &= \frac{dw_2(b)}{dx} \\ w_2(c) &= w_3(c) & \frac{dw_2(c)}{dx} &= \frac{dw_3(c)}{dx} \\ w_3(L-d) &= w_4(L-d) & \frac{dw_3(L-d)}{dx} &= \frac{dw_4(L-d)}{dx} \\ w_4(L-b) &= w_5(L-b) & \frac{dw_4(L-b)}{dx} &= \frac{dw_5(L-b)}{dx} \end{aligned} \quad (8-15)$$

The stiffness of a plate strip under this FPB configuration is defined as the total load $2P$ over the displacement at the loading points (note that $w_1(b) = w_2(b) = w_4(L-b) = w_5(L-b)$):

$$K = \frac{2P}{w_1(b)} \quad (16)$$

Finally, the total panel stiffness is simply the summation of all the individual strip stiffness contributions. While this analysis is specific to the four point bending test geometry, the methodology used in the analysis can be readily incorporated into buckling calculations due to its simplicity and mechanics based foundation.

Results

As shown in Table 2, the predictions of reduced bending stiffness (Predicted K) match fairly well with actual test measurements of bending stiffness (Measured K). The largest difference between Measured and Predicted K of 12% is found for specimen ICE-02B. Sources of error in predicting K lie in the mapping of the delamination zone and the assumptions made on the zone’s reduced bending stiffness value. However, considering these sources of error, in addition to the great simplifications made by the predictive methodology used, the results are surprisingly accurate. Predictions on the order of 10% are considered quite adequate for most design purposes.

Table 2. Comparison of Predicted to Measured Bending Stiffness for Delaminated Panels

Panel ID	Layup	Material	Thickness	Undamaged K	Measured K	Predicted K
ICE-01C	[0/45/90] _s	AS4/977 5HS	1.42 mm	117.0 KN/m	104.4 KN/m	106.3 KN/m
ICE-02B	[0/45/90/-45] _s	AS4/977 5HS	1.91	273.2	219.6	245.5
ICE-02C	[0/45/90/-45] _s	AS4/977 5HS	1.91	273.0	232.9	245.9
ICE-04E	[0/45] _s	AS4/8552 8HS	1.22	79.0	67.8	73.9
ICE-05A	[0/45/90] _s	AS4/8552 8HS	1.83	251.0	213.1	220.5
ICE-06D	[0/45/90/-45] _s	AS4/8552 8HS	2.44	579.0	502.9	484.7
ICE-06F	[0/45/90/-45] _s	AS4/8552 8HS	2.44	579.0	547.9	535.7

Application: Buckling Prediction

Having first been validated for an analytically simple form of loading, that is four point bending, the predictive methodology previously developed is now applied towards predicting the reduction in buckling critical load for impact damaged composite structures.

For a structure composed of thin skins stiffened by stringers, individual bays (plate region between stringers) can potentially undergo local buckling relative to the whole structure. As shown in Figure 4, a flat plate with simply supported boundaries is customarily used to model a single bay [9] when predicting the local buckling critical load.

As a gross simplification, the plates listed in Table 1 are treated as isotropic plates with “D” matrix (from Classical Lamination Plate Theory) terms $D_{11} = D_{22}$ and $D_{16}, D_{26} \ll D_{11}$. This assumption is good for the eight ply Quasi-Isotropic fabric specimens tested (ICE-02 and ICE-06 panels listed in Tables 1 and 2). Following Szilard [9], the critical buckling load for an isotropic square plate under uniaxial compressive loading is:

$$N_{cr} = \lambda N_{xo} = 4N_{xo} \quad (17)$$

Where $N_{xo} = \frac{\pi^2 D}{a^2}$ is the Euler buckling load for a single simply supported plate strip. a is the square plate size dimension, and D is the plate bending stiffness. λ is the buckling load factor which equals 4 for the case of predicting critical buckling load for an undamaged square plate. For simply supported square plates which contain impact damage, λ shall be less than 4.

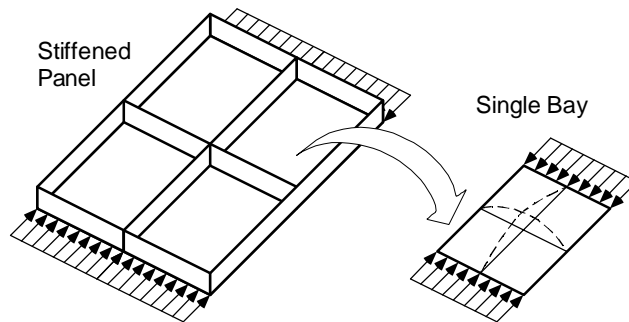


Figure 4. Single Bay Modeled From Stiffened Panel

A generic model of a plate with a rectangular zone of reduced bending stiffness is shown in Figure 5. The square zone of size a^* encompasses a region of damage such as the delamination shown here. For simplicity, the damage region is modeled with only a single rectangle. Further decomposition of the damage region into more strips is certainly possible, as well as implementable in the analytical methodology presented, for more accurate predictions.

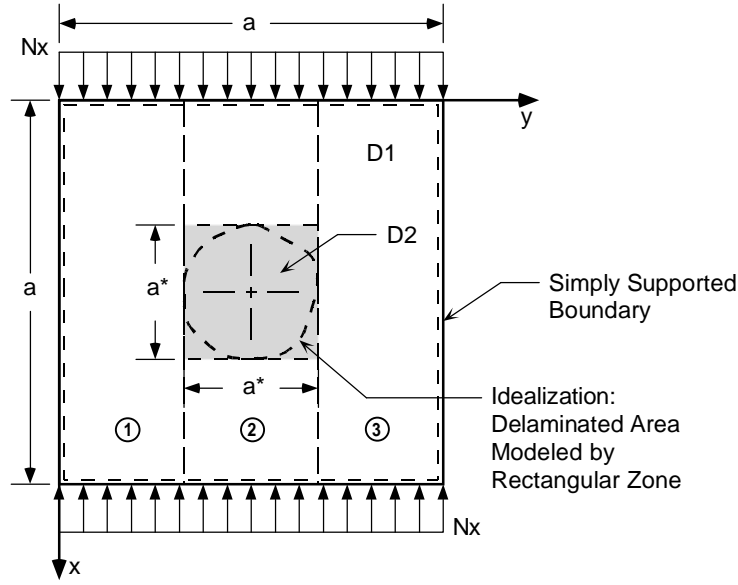


Figure 5. Model for Buckling Predictions

The model in Figure 5 is used to generate a simplified mechanics based prediction of the reduction in buckling load factor λ for impact delaminated structures. Two mechanics based models were developed. Both employ Rayleigh-Ritz's energy method for analysis which uses the total potential energy of a plate in the buckled state:

$$\Pi = \frac{1}{2} \iint_A D(x, y) \left\{ \left(\frac{\partial^2 w}{\partial x^2} \right)^2 + \left(\frac{\partial^2 w}{\partial y^2} \right)^2 - 2(1-\nu) \left[\frac{\partial^2 w}{\partial x^2} \frac{\partial^2 w}{\partial y^2} - \left(\frac{\partial^2 w}{\partial x \partial y} \right)^2 \right] \right\} dx dy - \frac{\lambda}{2} \iint_A N_{x0} \left(\frac{\partial w}{\partial x} \right)^2 dx dy \quad (18)$$

Note that the plate bending stiffness is a function of x and y . An assumed function for displacement:

$$w(x, y) = \sum_m \sum_n W_{mn} \sin \frac{m\pi x}{a} \sin \frac{n\pi y}{a} \quad (19)$$

is often used for a plate with simply supported boundaries. In the analyses, the simplest case of $m = 1, n = 1$ is used to model the first mode of plate buckling deformation. This simplifies Eqn 19 to:

$$w(x, y) = C \sin \frac{\pi x}{a} \sin \frac{\pi y}{a} \quad (20)$$

To determine the critical buckling load factor λ , Eqn 20 is substituted into Eqn 18, and the energy is minimized with respect to the single constant C .

Method 1. Rayleigh-Ritz Plate. Here Eqns 18 and 20 are directly applied to the model illustrated in Figure 5. The integrations are carried out piecewise over the domain:

$$\text{Let } U_i = D_i \left\{ \left(\frac{\partial^2 w}{\partial x^2} \right)^2 + \left(\frac{\partial^2 w}{\partial y^2} \right)^2 - 2(1-\nu) \left[\frac{\partial^2 w}{\partial x^2} \frac{\partial^2 w}{\partial y^2} - \left(\frac{\partial^2 w}{\partial x \partial y} \right)^2 \right] \right\} \quad i = 1, 2 \quad (21)$$

$$\begin{aligned} \Pi = & \frac{1}{2} \int_0^{\frac{1}{2}(a-a^*)} \int_0^a U_1 dx dy + \frac{1}{2} \int_{\frac{1}{2}(a-a^*)}^{\frac{1}{2}(a+a^*)} \left(\int_0^{\frac{1}{2}(a-a^*)} U_1 dx + \int_{\frac{1}{2}(a-a^*)}^{\frac{1}{2}(a+a^*)} U_2 dx + \int_{\frac{1}{2}(a+a^*)}^a U_1 dx \right) dy \\ & + \frac{1}{2} \int_{\frac{1}{2}(a+a^*)}^a \int_0^a U_1 dx dy - \frac{\lambda}{2} \iint_A N_{x0} \left(\frac{\partial w}{\partial x} \right)^2 dx dy \end{aligned} \quad (22)$$

Eqn 20 is substituted into Eqn 22 and upon minimizing the energy with respect to the constant C , the critical buckling load factor can be determined.

Method 2. Rayleigh-Ritz Strip. Figure 5 shows the plate to be divided into three separate strips, two of which contain no damage. An Euler column buckling analysis is performed on each strip using the model illustrated in Figure 6; D_1 and D_2 are the plate bending stiffness. For each strip, the critical buckling load is determined. The undamaged strips (1) and (3) have $D_1 = D_3 = D$, thus $N_{x_o,eff}^{(1,3)} = \frac{\pi^2 D}{a^2} = N_{x_o}$. For strip (2), $D_2 = D_1/4$ (as before in the FPB analyses) and $N_{x_o,eff}^{(2)}$ (which is $< N_{x_o}$) is determined by employing the Rayleigh-Ritz method simplified for the one-dimensional strip problem of Figure 6.

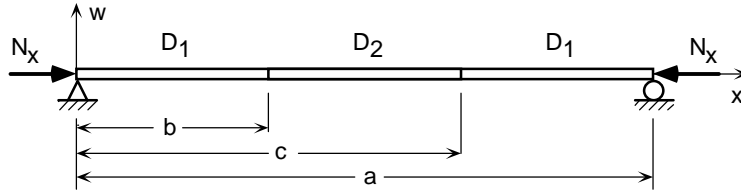


Figure 6. Rayleigh-Ritz Strip Model

Recalling Eqn 17, an assumption is made that the entire plate shall deform in the same manner as an undamaged simply supported plate. Furthermore, the reduction in total plate critical load shall be accounted for by modifying the strip critical load N_{x_o} . The calculation of λ is as follows:

$$N_{cr} = \lambda_{tot} N_{x_o} = 4N_{x_o, eff} \quad (23)$$

$$\text{where } N_{x_o, eff} = \frac{N_{x_o, eff}^{(2)} a^* + N_{x_o, eff}^{(1,3)} (a - a^*)}{a} \quad (24)$$

$$\text{thus } \lambda_{tot} = 4 \frac{N_{x_o, eff}}{N_{x_o}} \quad (25)$$

Note that $N_{x_o,eff}$ is determined by a simple “rule of mixtures” summation of the individual plate-strip Euler column buckling critical loads, scaled by the individual ratios of strip width to total width.

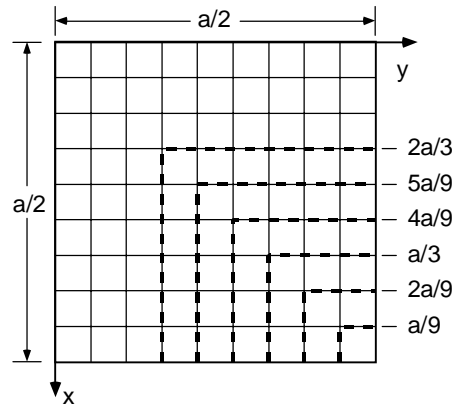


Figure 7. Finite Element Quarter Model

For validation of these predictive methods, a finite element model was created of a quarter plate with varying sized rectangular damage zones. Actual buckling tests of select panels are to be performed for more definite validation. The mesh and geometry of the finite element model is shown in Figure 7. Four node quadrilateral elements were used in the *ABAQUS* code to obtain eigenvalue buckling estimates.

The critical buckling load for damage zones of size $a^* = a/9$ to $2a/3$ were computed and comparisons made with the two analytical models. Figure 8 is a plot of the buckling load

factor reduction predictions made by the Rayleigh-Ritz Plate, Rayleigh-Ritz Strip, and the finite element models. The reduced load factor λ^* is reported relative to the undamaged load factor ($\lambda = 4$) as a function of the damage size ratio, a^*/a (see Figure 5). Surprisingly, the more simplistic Strip method predictions match more closely to the finite element. The Plate method predicts load factors which are consistently lower than the finite element and Strip methods.

Along side the buckling load factor reduction in Figure 8 are plotted the data points (reported in Table 2) for the predicted and measured reduced four point bending stiffness K^*/K . In addition to the reduced bending stiffness of actual damaged panels, predictions were made for panels with hypothetical square shaped damage zones identical in geometry to the buckling model in Figure 5. The analytical Strip method was used as well as finite element modeling to study the reduction in bending stiffness. The finite element model also serves as a comparison benchmark for the simplified methods used in predicting reduced bending stiffness. These results are plotted in Figure 8 as “FPB Hypothetical Strip” and “FPB Hypothetical FEM.” The Strip method predictions were in general lower than the finite element (by max. 4%). It is of interest to note the near 1:1 correlation between the predicted reduction in FPB stiffness and the predicted reduction in buckling load factor. Another point of interest is the identical reduction ratios predicted by the FPB finite element and the buckling Rayleigh-Ritz Strip method. The same reductions are predicted for entirely different cases of loading configuration as well as analytical formulation.

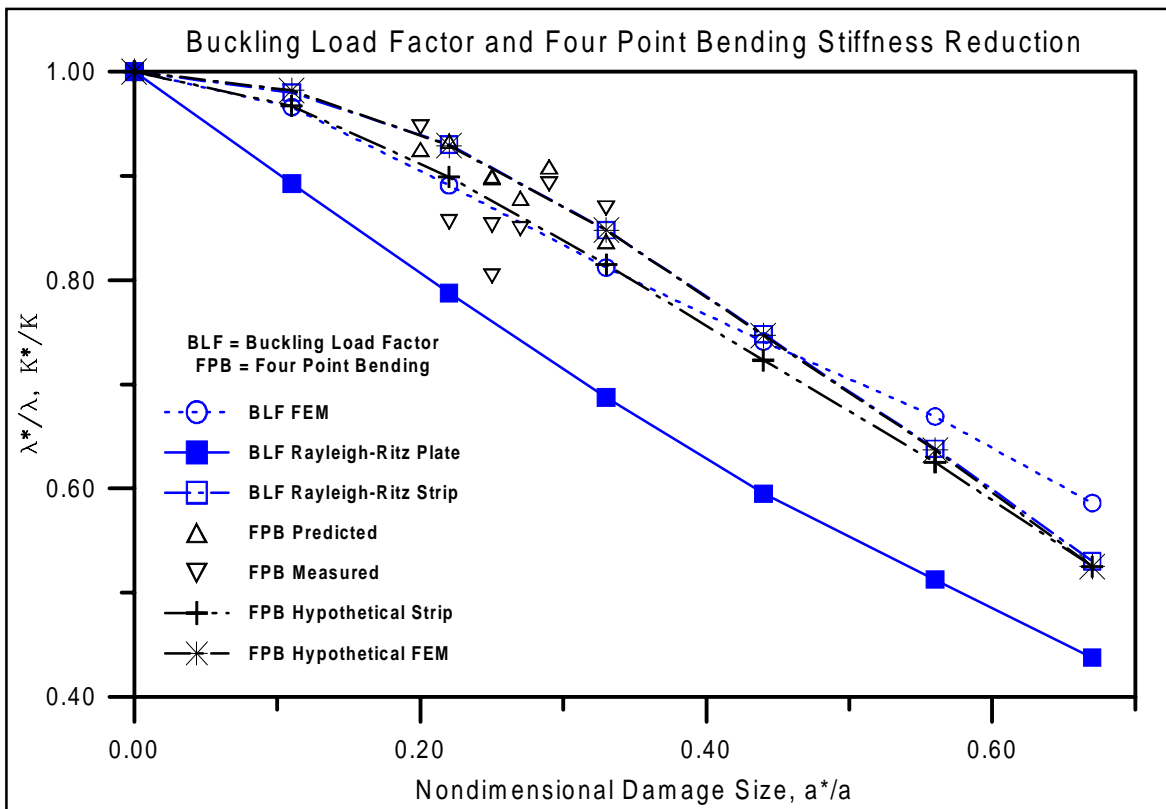


Figure 8. Comparison of Results for Buckling and Four Point Bending Reduction

Conclusions

A mechanics based predictive methodology has been developed to assess the effect of impact damage on composite structures. The method, although quite simplistic, accurately

predicted the reduction of four point bending stiffness for flat plates containing impact induced delamination damage. Applying the methodology to analytical buckling predictions, the method is found to predict the reduction in buckling critical load fairly well. Comparison of reduced buckling load and reduced bending stiffness, plotted versus damage size, shows a near 1:1 correlation between the two quantities. Reasons for the comparable trends are: the direct dependence of both the four point bending stiffness and the buckling critical load factor on the plate bending stiffness D , and the application of a bending moment field across the span of the plate; although moment varies along the length for the buckling problem. Additionally, functions used in describing the deformation shapes for first mode buckling and four point bending are identical.

While further investigation needs to be conducted into a broader set of buckling critical structures to investigate the range of applicability for the methodology developed herein, the results presented suggest that the use of four point bending tests are a simple means by which one can assess the reduction in buckling critical load for impact damaged composite plates. The methodology developed to predict the effects of impact damage on structural performance is applicable to many structures due to its mechanics based origins, thus facilitating the design of structures to be tolerant to known levels of impact damage.

Acknowledgments

The authors would like to acknowledge Douglas Welch, Gary Griesheim, Craig Musson, Chris Kogstrom, and Jeff Hill of United Technologies Pratt & Whitney for their assistance in the impact testing and their guidance towards maintaining the practical orientation of this research work.

References

1. Sjöblom, Peter. "Simple Design Approach Against Low Velocity Impact Damage," *International SAMPE Symposium and Exhibition*. Vol. 32. April 6-9, 1987.
2. Presentation by Philip Barkan, Professor of Mechanical Engineering, Stanford University.
3. Wilkins, D.J. "Compression Buckling Tests of Laminated Graphite-Epoxy Curved Panels," *AIAA Journal*, Vol. 13, No. 4, April 1975. pp. 465-470.
4. Chen, V.L., Wu X.X. and Sun C.T. "Prediction of Buckling Loads of Stiffened Composite Panels," *Proceedings of ASME Winter Annual*. Dallas, TX. Nov. 1990.
5. Kim, H., Welch, D.A. "Investigation of Hail Ice Impact on Composite Structures," *Pratt & Whitney Internal Report*. EII No. 95-200-0035-B. 1995.
6. Wisnom, Michael R. "Limitations of Linear Elastic Bending Theory Applied to Four Point Bending of Unidirectional Carbon Fibre-Epoxy," *AIAA-90-0960-CP*, 1990.
7. Grédiac, Michel. "Four-Point Bending Tests on Off-Axis Composites," *Composite Structures*, Vol. 24, 1993. pp. 89-98.
8. Adler, William F. and Mihora, Dennis J. "Biaxial Flexure Testing: Analysis and Experimental Results," *Fracture Mechanics of Composites*, Vol. 10. New York 1992. pp. 227-245.
9. Szilard, R. *Theory and Analysis of Plates, Classical and Numerical Methods*. Prentice-Hall, New Jersey, 1974.
10. ASTM Standards. "Standard Test Methods for Flexural Properties of Unreinforced and Reinforced Plastics and Electrical Insulating Materials," ASTM D790-92.